Supporting Information

Powell et al. 10.1073/pnas.1310655110

SI Methods

Mouse Repeated Social Defeat and Proinflammatory Monocytes. Male C57BL/6 mice between the ages of 6 and 8 wk (Charles River Laboratories) were allowed to acclimate to the animal facility for 1 wk before study procedures. Mice were housed in groups of three per cage and maintained on a 12-h light/dark schedule with the lights on at 0600 hours in an American Association of Accreditation of Laboratory Animal Care accredited facility. Food and water were available ad libitum. Animals were randomized to repeated social defeat (RSD) or home-cage control (HCC) conditions, as previously described (1–3). RSD involved introduction of aggressive intruder male mice into cages of established cohorts of three male mice for 2 h between 1630 and 1830 hours for six consecutive nights. At the end of the 2-h period, the aggressor was removed and the residents were left undisturbed until the following day when RSD was repeated. HCC mice were housed in a separate room and left undisturbed (except for parallel drug administrations as described below) until the day of cell harvest. Following the sixth cycle of RSD, circulating blood was collected by cardiac puncture for isolation of peripheral blood mononuclear cells (PBMCs); bone marrow mononuclear cells (BMMCs) were eluted from the femoral medulla; and total spleen cells were macerated to a single-cell suspension (3). All procedures were approved by The Ohio State University Institutional Animal Care and Use Committee.

Transcriptome profiling. In initial transcriptome surveys (Fig. 1*A*), $CD11b^+$ cells (>96% pure as determined by flow cytometry) were isolated from spleen cell suspensions by immunomagnetic positive selection (Miltenyi Biotec), and monocytes were retained by plastic adherence [2-h incubation of cells at 10^7/mL in plastic tissue culture flask at 37 °C in 5% (vol/vol) CO_2]. Total RNA was extracted (RNeasy; Qiagen), quantified by spectrophotometry (NanoDrop ND-1000; Thermo Scientific), and assessed for integrity by capillary electrophoresis (Bioanalyzer 2100; Agilent Inc.). Splenic monocyte samples from HCC mice yielded insufficient RNA for individual assay, so samples were pooled in groups of two for assay. A total of 5 μg of total RNA was assayed using Affymetrix MOE430 2.0 high-density oligonucleotide arrays (4) in the University of California, Los Angeles (UCLA) DNA Microarray Core as previously described (5–7). Robust multiarray averaging (8) was applied to quantify expression of 45,068 assayed transcripts, and differentially expressed genes were identified by ≥50% difference in mean ($\log_2$) expression levels in cells from RSD vs. HCC animals (corresponding to a false discovery rate of 5%) (5). Differentially expressed genes were identified based on biological effect size (i.e., difference = $\text{mean}_{RSD} - \text{mean}_{HCC}$) rather than statistical effect size (e.g., *t* statistic or *P* value) because previous research has shown that biological effect size-based criteria yield more replicable results than do statistical effect size criteria (e.g., *t* statistics, *P* values, or false discovery rate *q* values) (5, 9–11). Differentially expressed genes are listed in Dataset S1, and gene expression data are deposited in the National Center for Biotechnology Information Gene Expression Omnibus (GEO; accession no. GSE28830).

Confirmatory RT-PCR. Ten gene transcripts characteristic of key biological functions of immature, proinflammatory monocytes (inflammation, proliferation, and differentiation) were selected for independent verification of differential expression by quantitative real-time RT-PCR using TaqMan Gene Expression Assays (Applied Biosystems Inc.) for mouse *Arg2*, *Ccr1*, *Ceacam10*, *Mmp9*, *Mpo*, *Myc*, *Ptges*, *Ptgfrn*, *Sod2*, *Tgfb*, *Gapdh*, and *18s* RNA. Assays were performed on an Applied Biosystems real-time PCR instrument using standard procedures previously described (12, 13), and mRNA abundance was derived from standard threshold cycle number analysis after normalization of values for each target transcript to the average of *18s* and *Gapdh* threshold cycle numbers. Results confirmed >50% differential expression for eight of the 10 target genes assayed. Microarray results were also validated by consistency with previously published RSD experiments assessing $CD11b^+$ cell expression of mRNA and/or protein levels of IL-1β, IL-6, TNF-α, and IFN-γ (1, 12, 14–19). Also consistent with previous observations (12, 16, 20), the GR *Nr3c1* gene was expressed at comparable levels in monocytes from RSD vs. HCC animals (3% difference in average expression across five *Nr3c1* probe sets on the MOE430 2.0 array; difference $P = 0.457$). This finding provides a negative control indicating no difference in microarray-derived gene expression when no difference would be expected based on previous protein- and RNA-based studies (12, 16, 20).

Transcription control pathway analysis. We used a two-sample variant of the Transcription Element Listening System (TELiS; www.telis.ucla.edu) (6) to compare the prevalence of transcription factor-binding motifs (TFBMs) from the TRANSFAC database (21) in promoters of genes overexpressed in cells from RSD- vs. HCC-treated animals (Fig. 2*C*). Primary analyses tested activity of the myeloid differentiation transcription factor PU.1 [marked by the consensus E-twenty six (ETS) family transcription factor motif V$ELK1_02]; transcription factors involved in expression of immune response effector genes, including NF-κB (V$CREL_01), EGR1 (V$EGR1_01), MZF1 (V$MZF1_01), and the redox-responsive transcription factor NRF2 (V$NRF2_01); and transcription factors involved in terminal differentiation of myeloid cells, including E2-2 (V$E2_01) and Gfi1 (V$GFI_01); factors specifying dendritic cell fate; and cMaf/MafB (V$VMAF_01), CREB (V$CREB_01), and AP-1 (V$AP1_C) factors linked to macrophage differentiation (22–25). Analyses of glucocorticoid insensitivity compared the prevalence of V$GR_Q6 TFBMs in promoters of genes overexpressed in cells from RSD- vs. HCC-treated animals (7, 26, 27). In each case, initial analyses defined promoters as nucleotide sequences spanning the region −600 bp to +0 bp relative to the gene transcription start site (6) and detected TFBMs using a MatSim match stringency of 0.80 (28). Additional sensitivity analyses averaged results derived from nine parametric variations of promoter length (−300 bp relative to RefSeq transcription start site, −600 bp, and −1000 bp to +200) and target TFBM match stringency (MatSim = 0.80, 0.90, 0.95) (6). Differential TFBM prevalence was assessed by two-tailed *P* values from a paired-sample *t* test (29).

Transcriptome representation analysis. To quantify group differences in the prevalence of the Ly-$6c^{high}$ monocyte transcriptome within the total mouse monocyte pool, we analyzed differential expression of genes that empirically showed substantial differential expression between Ly-$6c^{high}$ and Ly-$6c^{low}$ monocytes in a previous reference study of isolated monocyte subsets. A set of cell type-diagnostic transcripts was defined by ≥6 SD difference in average ($\log_2$) expression in genome-wide transcriptional profiling of isolated mouse Ly-$6c^{high}$ and Ly-$6c^{low}$ monocytes from GEO accession no. GSE17256 (30), and these cell type-diagnostic transcripts were then tested in the present study for differential representation in RSD vs. HCC total monocyte samples by a paired-sample *t* test (29) (individual gene results are listed in Dataset S2). This transcriptome representation analysis (TRA) assesses differential expression of genes previously identified as highly diagnostic of a given cell type in a separate validation sample (i.e., differential expression in the present study | cell type diagnosticity ≥ threshold

d in the previous reference study). In contrast, the previously published transcript origin analysis (TOA) (27) tests the cell type diagnosticity of genes already identified as differentially expressed (i.e., cell type diagnosticity in previous reference study | differential expression ≥ threshold d in the present study). TOA seeks to identify the cell type(s) contributing to observed differences in gene expression within a heterogeneous RNA pool, regardless of whether those differences stem from per-cell changes in gene expression or differential prevalence of total cell transcriptomes (i.e., differential cell type prevalence). Because TRA tests differential expression of all genes previously identified as highly diagnostic of a given cell type, this approach is insensitive to per-cell changes in expression of selected genes, and is highly sensitive to correlated variation in the relative prevalence of all genes within a given cellular transcriptome (i.e., TRA is primarily sensitive to variations in total cell transcriptome prevalence).

Confirmatory PBMC transcriptome profiling and monocyte-depletion analysis. To determine whether monocytes in particular mediate the effects of RSD on proinflammatory gene expression within the total PBMC pool, we carried out confirmatory transcriptome profiling on total PBMC samples and parallel PBMC samples from which $CD11b^+$ cells (monocytes) were depleted by immunomagnetic negative selection (Miltenyi Biotec). In each of three separate experiments, three mice were randomized to six cycles of RSD or parallel HCC conditions as described above, and PBMCs were obtained from cardiac puncture blood samples subject to standard KCl red blood cell lysis. From samples of 10^6 PBMCs and CD11b-depleted PBMCs (>98% purity; i.e., <2% $CD11b^+$ cells as determined by flow cytometry), total RNA was extracted (Qiagen RNeasy), quantified by spectrophotometry (NanoDrop ND-1000), and assessed for integrity by capillary electrophoresis (Agilent Bioanalyzer 2100). All samples met quality assurance criteria and were subject to transcriptome profiling by Illumina MouseRef-8 BeadArrays according to the manufacturer's standard protocol (Illumina Inc.) in the UCLA Neuroscience Genomics Core, as previously described (27). Data are deposited in GEO accession no. GSE47154. Expression values for 18,118 assayed genes were quantile normalized and $\log_2$ transformed for assessment of differential gene expression as the difference between average expression values for RSD vs. HCC conditions (i.e., difference = $\text{mean}_{\text{RSD}} - \text{mean}_{\text{HCC}}$). Linear difference scores were back-transformed for presentation as a fold difference in gene expression (i.e., fold-difference = $2^{\text{difference}}$). To assess the extent to which $CD11b^+$ cells mediated the general transcriptomic effect of RSD on the total PBMC pool, the general transcriptomic effect of RSD was defined as the average change in expression for the top 100 genes showing the largest magnitude of RSD-induced up-regulation in PBMCs (i.e., the top 100 values of $\text{difference}_{\text{PBMC}}$). Differential expression of the same genes was quantified in parallel in CD11b-depleted PBMC (i.e., $\text{difference}_{\text{PBMC-CD11b}}$), and the statistical significance of the difference in RSD-induced transcriptome alteration in total PBMCs vs. CD11b-depleted PBMCs was assessed in a mixed-effect linear model (31) analysis of gene expression values for the top 100 RSD up-regulated genes as a function of gene-specific differences in average expression level (treated as a repeated measure), experimental condition (RSD vs. HCC), cell population (total PBMCs vs. CD11b-depleted PBMCs), and the interaction of experimental condition × cell population (the parameter representing the target of analysis, i.e., capturing the magnitude of difference in RSD effect on gene expression in total PBMCs vs. CD11b-depleted PBMCs). Following the identification of a statistically significant overall experimental condition × cell population interaction, the pattern of differential RSD results was defined in follow-up simple effects analyses of experimental condition (difference = $\text{mean}_{\text{RSD}} - \text{mean}_{\text{HCC}}$) nested within cell population (total PBMCs or CD11b-depleted PBMCs). All models were fit using SAS PROC MIXED (SAS 9.3; SAS Institute), with estimated means and SEs back-transformed to a linear (fold difference) metric for presentation in Fig. 1*B* as described above. Fig. 1*B* also presents results for six individual representative proinflammatory genes within the top 100 up-regulated genes (*Ly6c*, *Il1b*, *Myd88*, *Tlr2*, *Fos*, *Il8rb*). Throughout all analyses, all P values are two-tailed, and $P < 0.05$ serves as the threshold of statistical significance.

Flow cytometry. Prevalence of $CD11b^+/Gr1^+/Ly\text{-}6c^{high}$ monocytes was assessed in BMMCs, circulating PBMCs, and splenocytes by flow cytometry as described previously (13, 17, 18). Briefly, 2.5×10^5 cells were incubated at 4 °C for 45 min with FITC-conjugated Abs to mouse Ly-6c, PE-conjugated Abs to mouse Gr1, and APC-conjugated Abs to mouse CD11b (all Abs from BD Biosciences). Samples were subsequently washed twice in FACS buffer, and fluorescence intensity data were acquired for 10,000 lymphocyte-gated events on a FACSCalibur instrument (BD Biosciences). Compensation and isotype and negative controls were used to control for background and for instrument set-up. Results were analyzed using FlowJo (Tree Star Inc.) or CellQuest software (BD Biosciences) with leukocytes gated based on forward- vs. side-scatter profiles, monocytes gated within the leukocyte population based on $CD11b^+/Gr1^+$ immunofluorescence, and $Ly\text{-}6c^{high}$ vs. $Ly\text{-}6c^{low}$ monocyte phenotypes subsequently gated within the $CD11b^+/Gr1^+$ monocyte population. Similar analyses were carried out on BMMCs to identify mixed-lineage progenitor cells and cells committed to lymphoid, erythroid, granulocytic, and monocytic lineages based on Ly-6c–FITC and CD31–PE immunofluorescence (32, 33). Differences between RSD and HCC conditions were analyzed using Welch two-sample t tests (29).

β-Adrenergic regulation of proinflammatory gene expression. To determine the role of β-adrenergic signaling in RSD-induced up-regulation of proinflammatory gene expression in peripheral blood monocytes, mice were injected s.c. with 10 mg/kg propranolol (Sigma) in saline containing 0.2% ethanol, or the same volume of vehicle, 30 min before each cycle of RSD (or at a parallel time point under HCC conditions) in a 2 (experimental condition: RSD vs. HCC) × 2 (drug: propranolol vs. vehicle) factorial design with $n = 3$ mice per condition in each of four independent experiments. This dose has been empirically shown to optimize functional β-blockade in previous studies of the mouse RSD paradigm (34). Following six cycles of RSD (or parallel HCC conditions), peripheral blood $CD11b^+$ monocytes were isolated from cardiac puncture blood samples and subject to transcriptome profiling using Illumina MouseRef-8 BeadArrays as described in *Confirmatory PBMC transcriptome profiling and monocyte-depletion analysis*. Data are deposited in GEO accession no. GSE47154. Seventeen genes were selected a priori as representative proinflammatory transcripts based on Gene Ontology and EntrezGene functional annotations of proinflammatory chemokine activity (*Cxcl1*, *Cxcl2*), AP-1 signaling (*Fos*, *Fosb*, *Fosl1*, *Jun*, *Junb*, *Jund1*), proinflammatory cytokine activity (*Il1a*, *Il1b*, *Il6*, *Tnf*), inflammatory prostaglandin synthesis (*Ptgs1*, *Ptgs2*), Toll-like receptor signaling (*Myd88*, *Tlr2*), and proinflammatory monocyte phenotyping markers (*Ly6c*, *Tlr2*). Log_2-transformed expression values for these genes were analyzed in a mixed-effect linear model (31), including parameters representing gene-specific differences in average expression (treated as a repeated measure), experimental condition (RSD vs. HCC), drug (propranolol vs. vehicle control), and the interaction of experimental condition × drug (the primary target of analysis, testing the extent to which propranolol abrogated RSD-induced up-regulation of proinflammatory gene expression). Following the identification of a statistically significant overall experimental condition × drug interaction, the pattern of differential RSD effects was defined in follow-up simple effects analyses of experimental condition (difference = $\text{mean}_{\text{RSD}} - \text{mean}_{\text{HCC}}$) nested within drug (propranolol vs. vehicle control). All models were fit using SAS PROC MIXED, with estimated means and SEs

back-transformed to a linear (fold difference) metric for presentation in Fig. 3*D* as described above.

Role of myelopoietic growth factors GM-CSF and M-CSF. To determine whether the myelopoietic growth factor GM-CSF might mediate RSD-induced up-regulation of myelopoiesis, RSD and HCC mice were injected s.c. with either 300 μg of anti-mouse GM-CSF–neutralizing antibody MP1-22E9 or an equivalent volume of isotype control IgG2a κ antibody (eBioscience) at 48-h intervals starting 1 d before RSD. This dose of MP1-22E9 has been shown to block biological activity of GM-CSF in multiple in vivo mouse models of immune function and disease (35–37). In three separate experiments, $n = 8$ mice per condition were randomized to six cycles of RSD or parallel HCC conditions in a 2 (experimental condition: RSD vs. HCC) × 2 (drug: anti–GM-CSF vs. isotype control) factorial design. Following six cycles of RSD (or parallel HCC conditions), PBMC and BMMC samples were assayed as described above (flow cytometry) to assess prevalence of $CD11b^{+}/Ly\text{-}6c^{high}$ monocytes and $CD11b^{+}/Ly\text{-}6c^{intermediate}$ granulocytes (in PBMCs) and $CD31^{+}/Ly\text{-}6c^{high}$ monocyte precursors and $CD31^{+}/Ly\text{-}6c^{intermediate}$ granulocyte precursors (in BMMCs). The percentage of each cell type within the total mononuclear cell population was analyzed in a factorial analysis of variance model (29), including parameters representing the effects of experimental condition (RSD vs. HCC), drug (anti–GM-CSF vs. isotype control), and the interaction of experimental condition × drug (the primary target of analysis testing the extent to which anti–GM-CSF abrogated RSD-induced up-regulation of myelopoiesis). Following the identification of a statistically significant overall experimental condition × drug interaction, the pattern of differential RSD effects was defined in simple effects analyses of experimental condition (difference = $mean_{RSD} - mean_{HCC}$) nested within drug condition (anti–GM-CSF vs. isotype control). Data were analyzed using SAS PROC GLM, with estimated means and SEs presented in Fig. 3 *E* and *F*.

To determine whether the myelopoietic growth factor M-CSF might mediate RSD-induced up-regulation of monopoiesis, we carried out studies parallel to those described above using 160 mg/kg of the M-CSF receptor (CSF1R) antagonist GW2580 [5-(3-methoxy-4-[(4-methoxybenzyl)oxy]benzyl)-pyrimidine-2,4-diamine] (Rhode Island Chemical) or an equivalent volume of vehicle (0.5% hydroxypropyl methylcellulose, 0.1% Tween 20; Sigma). GW2580 was administered daily by oral gavage beginning 24 h before RSD. This dosing regimen has been shown to block multiple monocyte-dependent immunologic processes and disease parameters in in vivo mouse models (38–44). Following six cycles of RSD (or parallel HCC conditions), PBMC monocyte and granulocyte populations and BMMC monocytic and granulocytic progenitor cell populations were quantified by flow cytometry and subject to statistical analysis as described above.

Human Socioeconomic Status and Proinflammatory Monocytes.

Sample and design. Data are from a previously detailed gene expression study of PBMC samples from 60 adults recruited from Vancouver through postings in local media and public transit (45, 46). Demographic and behavioral characteristics of the sample have been previously reported (45, 46). To be eligible, participants had to be 25–40 y of age and in good health (no history of chronic disease and free of infection for the past 4 wk). Participant socioeconomic status (SES) was defined by occupational status over the past 5 y (low SES: routine, manual, or lower supervisory occupations; high SES: managerial or professional occupations; with participant SES defined by the higher of either participant's or romantic partner's occupational status) using the United Kingdom's National Statistics Socioeconomic Classification (47). Age, sex, race, and smoking were measured using established self-report instruments, and body mass index (BMI) was determined from directly measured height and weight (45, 46). The project was approved by the University of British Columbia's Research Ethics Board, and all subjects gave written consent before participating.

Transcriptome profiling. PBMCs were isolated from whole blood through density-gradient centrifugation, lysed in RNA stabilization buffer (Qiagen RLT), homogenized (Qiagen QiaShredder), and frozen at −80 °C for subsequent gene expression profiling in batch. At gene expression profiling, RNA was extracted using AllPrep DNA/RNA kits (Qiagen); RNA purity and integrity were verified using an Agilent 2100 Bioanalyzer; and 50 ng of total RNA was assayed on an Illumina BeadStation 500 using HumanRef-8 v3.0 Expression BeadArrays (Illumina) following the manufacturer's standard protocol in the Genome Quebec Innovation Centre (Montreal). Raw expression values were $\log_2$ transformed, and differentially expressed genes were identified by ≥20% difference in mean expression levels between low- and high-SES groups (following thresholds used in previous analyses of this dataset) (45, 46) in multiple regression models controlling for age, sex, race, BMI, and smoking. Data are deposited in GEO accession no. GSE15180. To assess the role of the β-adrenergic transcription factor CREB in structuring the observed differences in gene expression, we conducted TELiS promoter-based bioinformatics analyses (6) as described above (*Transcription Control Pathway Analysis*) using the TRANSFAC V$CREB_01 position-specific weight matrix (21). The cellular origins of differentially expressed genes were inferred by TOA using PBMC constituent reference cell populations [monocyte, plasmacytoid dendritic cell, $CD4^{+}$ T-cell, $CD8^{+}$ T-cell, B-cell, and natural killer (NK) cell] as described previously (27). Parallel aliquots of whole blood were analyzed by Coulter Counter to quantify the absolute numbers and relative percentages of monocytes, lymphocytes, eosinophils, basophils and neutrophils.

Transcriptome representation analysis. To quantify group differences in the prevalence of total monocytes and the $CD16^{-}$ monocyte subset within the total PBMC pool, we conducted TRA as described above. In analyses of the $CD16^{-}$ monocyte subset, cell type-diagnostic genes were defined by a standardized difference (Cohen's d) ≥6 SD in average transcript abundance within isolated human $CD16^{-}$ vs. $CD16^{+}$ monocytes from GEO accession no. GSE18565 (30). In analyses of overall monocyte prevalence within the PBMC pool, cell type diagnosticity was defined as a score ≥6 SD on a standardized expression index previously shown to identify transcripts expressed specifically by monocytes in comparison with parallel-isolated populations of plasmacytoid dendritic cells, NK cells, B cells, $CD4^{+}$ T cells, and $CD8^{+}$ T cells in transcriptome profiling of human leukocyte subsets from GEO accession no. GSE1133 (27, 48). In both analyses, paired t tests assessed differences in average expression of cell type-diagnostic transcripts within PBMC samples from the present low-SES vs. high-SES groups (29). In these analyses, all reported P values are two-tailed, and $P < 0.05$ constitutes the threshold of statistical significance.

1. Avitsur R, Kavelaars A, Heijnen C, Sheridan JF (2005) Social stress and the regulation of tumor necrosis factor-alpha secretion. *Brain Behav Immun* 19(4):311–317.
2. Bailey MT, Engler H, Powell ND, Padgett DA, Sheridan JF (2007) Repeated social defeat increases the bactericidal activity of splenic macrophages through a Toll-like receptor-dependent pathway. *Am J Physiol Regul Integr Comp Physiol* 293(3):R1180–R1190.
3. Powell ND, et al. (2009) Repeated social defeat activates dendritic cells and enhances Toll-like receptor dependent cytokine secretion. *Brain Behav Immun* 23(2):225–231.
4. Lockhart DJ, et al. (1996) Expression monitoring by hybridization to high-density oligonucleotide arrays. *Nat Biotechnol* 14(13):1675–1680.
5. Cole SW, Galic Z, Zack JA (2003) Controlling false-negative errors in microarray differential expression analysis: A PRIM approach. *Bioinformatics* 19(14):1808–1816.
6. Cole SW, Yan W, Galic Z, Arevalo J, Zack JA (2005) Expression-based monitoring of transcription factor activity: The TELiS database. *Bioinformatics* 21(6):803–810.
7. Cole SW, et al. (2010) Computational identification of gene-social environment interaction at the human IL6 locus. *Proc Natl Acad Sci USA* 107(12):5681–5686.

8. Bolstad BM, Irizarry RA, Astrand M, Speed TP (2003) A comparison of normalization methods for high density oligonucleotide array data based on variance and bias. *Bioinformatics* 19(2):185–193.
9. Witten DM, Tibshirani R (2007) *A Comparison of Fold-Change and the t-Statistic for Microarray Data Analysis* (Stanford University, Stanford, CA). Available at www-stat.stanford.edu/~tibs/ftp/daniela-fold.pdf. Accessed November 9, 2011.
10. Shi L, et al.; MAQC Consortium (2010) The MicroArray Quality Control (MAQC)-II study of common practices for the development and validation of microarray-based predictive models. *Nat Biotechnol* 28(8):827–838.
11. Shi L, et al. (2008) The balance of reproducibility, sensitivity, and specificity of lists of differentially expressed genes in microarray studies. *BMC Bioinformatics* 9(Suppl 9): S10.
12. Bailey MT, et al. (2009) Social stress enhances allergen-induced airway inflammation in mice and inhibits corticosteroid responsiveness of cytokine production. *J Immunol* 182(12):7888–7896.
13. Mays JW, et al. (2010) Influenza virus-specific immunological memory is enhanced by repeated social defeat. *J Immunol* 184(4):2014–2025.
14. Quan N, et al. (2001) Social stress increases the susceptibility to endotoxic shock. *J Neuroimmunol* 115(1-2):36–45.
15. Stark JL, Avitsur R, Hunzeker J, Padgett DA, Sheridan JF (2002) Interleukin-6 and the development of social disruption-induced glucocorticoid resistance. *J Neuroimmunol* 124(1-2):9–15.
16. Engler H, et al. (2008) Interleukin-1 receptor type 1-deficient mice fail to develop social stress-associated glucocorticoid resistance in the spleen. *Psychoneuroendocrinology* 33(1):108–117.
17. Kinsey SG, Bailey MT, Sheridan JF, Padgett DA (2008) The inflammatory response to social defeat is increased in older mice. *Physiol Behav* 93(3):628–636.
18. Bailey MT, Kinsey SG, Padgett DA, Sheridan JF, Leblebicioglu B (2009) Social stress enhances IL-1beta and TNF-alpha production by *Porphyromonas gingivalis* lipopolysaccharide-stimulated CD11b+ cells. *Physiol Behav* 98(3):351–358.
19. Curry JM, et al. (2010) Social disruption induces lung inflammation. *Brain Behav Immun* 24(3):394–402.
20. Quan N, et al. (2003) Molecular mechanisms of glucocorticoid resistance in splenocytes of socially stressed male mice. *J Neuroimmunol* 137(1-2):51–58.
21. Wingender E, Dietze P, Karas H, Knüppel R (1996) TRANSFAC: A database on transcription factors and their DNA binding sites. *Nucleic Acids Res* 24(1): 238–241.
22. Geissmann F, et al. (2010) Development of monocytes, macrophages, and dendritic cells. *Science* 327(5966):656–661.
23. Valledor AF, Borràs FE, Cullell-Young M, Celada A (1998) Transcription factors that regulate monocyte/macrophage differentiation. *J Leukoc Biol* 63(4):405–417.
24. Saeki K, Saeki K, Yuo A (2003) Distinct involvement of cAMP-response element-dependent transcriptions in functional and morphological maturation during retinoid-mediated human myeloid differentiation. *J Leukoc Biol* 73(5):673–681.
25. Sawka-Verhelle D, et al. (2004) PE-1/METS, an antiproliferative Ets repressor factor, is induced by CREB-1/CREM-1 during macrophage differentiation. *J Biol Chem* 279(17): 17772–17784.
26. Cole SW, et al. (2007) Social regulation of gene expression in human leukocytes. *Genome Biol* 8(9):R189.
27. Cole SW, Hawkley LC, Arevalo JM, Cacioppo JT (2011) Transcript origin analysis identifies antigen-presenting cells as primary targets of socially regulated gene expression in leukocytes. *Proc Natl Acad Sci USA* 108(7):3080–3085.
28. Quandt K, Frech K, Karas H, Wingender E, Werner T (1995) MatInd and MatInspector: New fast and versatile tools for detection of consensus matches in nucleotide sequence data. *Nucleic Acids Res* 23(23):4878–4884.
29. Miller RG (1986) *Beyond ANOVA: Basics of Applied Statistics* (Wiley, New York).
30. Ingersoll MA, et al. (2010) Comparison of gene expression profiles between human and mouse monocyte subsets. *Blood* 115(3):e10–e19.
31. McCulloch CE, Searle SR, Neuhaus JM (2008) *Generalized, Linear, and Mixed Models* (Wiley, Hoboken, NJ).
32. Leenen PJ, Slieker WA, Melis M, Van Ewijk W (1990) Murine macrophage precursor characterization. I. Production, phenotype and differentiation of macrophage precursor hybrids. *Eur J Immunol* 20(1):15–25.
33. Nikolic T, de Bruijn MF, Lutz MB, Leenen PJ (2003) Developmental stages of myeloid dendritic cells in mouse bone marrow. *Int Immunol* 15(4):515–524.
34. Wohleb ES, et al. (2011) β-Adrenergic receptor antagonism prevents anxiety-like behavior and microglial reactivity induced by repeated social defeat. *J Neurosci* 31(17):6277–6288.
35. Plater-Zyberk C, et al. (2007) GM-CSF neutralisation suppresses inflammation and protects cartilage in acute streptococcal cell wall arthritis of mice. *Ann Rheum Dis* 66(4):452–457.
36. Puljic R, et al. (2007) Lipopolysaccharide-induced lung inflammation is inhibited by neutralization of GM-CSF. *Eur J Pharmacol* 557(2-3):230–235.
37. Vlahos R, et al. (2010) Neutralizing granulocyte/macrophage colony-stimulating factor inhibits cigarette smoke-induced lung inflammation. *Am J Respir Crit Care Med* 182(1):34–40.
38. Sloan EK, et al. (2010) The sympathetic nervous system induces a metastatic switch in primary breast cancer. *Cancer Res* 70(18):7042–7052.
39. Priceman SJ, et al. (2010) Targeting distinct tumor-infiltrating myeloid cells by inhibiting CSF-1 receptor: Combating tumor evasion of antiangiogenic therapy. *Blood* 115(7):1461–1471.
40. Conway JG, et al. (2005) Inhibition of colony-stimulating-factor-1 signaling in vivo with the orally bioavailable cFMS kinase inhibitor GW2580. *Proc Natl Acad Sci USA* 102(44):16078–16083.
41. Menke J, et al. (2012) Autocrine CSF-1 and CSF-1 receptor coexpression promotes renal cell carcinoma growth. *Cancer Res* 72(1):187–200.
42. Crespo O, et al. (2011) Tyrosine kinase inhibitors ameliorate autoimmune encephalomyelitis in a mouse model of multiple sclerosis. *J Clin Immunol* 31(6): 1010–1020.
43. Paniagua RT, et al. (2010) c-Fms-mediated differentiation and priming of monocyte lineage cells play a central role in autoimmune arthritis. *Arthritis Res Ther* 12(1):R32.
44. Shaposhnik Z, Wang X, Lusis AJ (2010) Arterial colony stimulating factor-1 influences atherosclerotic lesions by regulating monocyte migration and apoptosis. *J Lipid Res* 51(7):1962–1970.
45. Chen E, Miller GE, Kobor MS, Cole SW (2011) Maternal warmth buffers the effects of low early-life socioeconomic status on pro-inflammatory signaling in adulthood. *Mol Psychiatry* 16(7):729–737.
46. Miller GE, et al. (2009) Low early-life social class leaves a biological residue manifested by decreased glucocorticoid and increased proinflammatory signaling. *Proc Natl Acad Sci USA* 106(34):14716–14721.
47. Office of National Statistics (2005) *The National Statistics Socio-Economic Classification* (Palgrave Macmillan, Hampshire, UK).
48. Su AI, et al. (2004) A gene atlas of the mouse and human protein-encoding transcriptomes. *Proc Natl Acad Sci USA* 101(16):6062–6067.

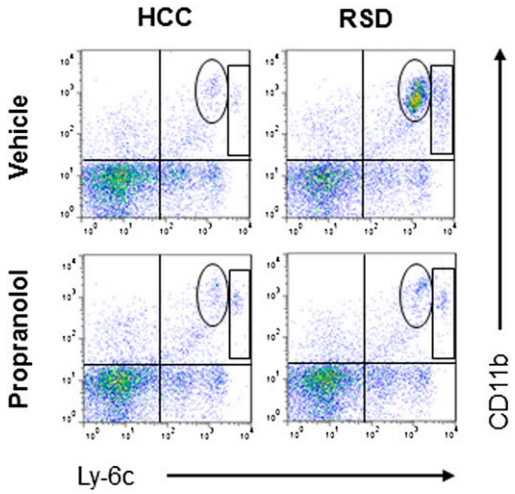

Fig. S1. Role of β-adrenergic signaling in RSD effects on monocyte and granulocyte prevalence. To determine whether RSD effects on peripheral myeloid cell prevalence were mediated by β-adrenergic signaling, mice received an i.p. injection of propranolol (or an equivalent volume of saline vehicle) once daily before experimental procedures. Following six cycles of RSD or parallel HCC conditions, total splenocytes were assayed by flow cytometry for prevalence of Ly-6c^{high}/CD11b^{+} monocytes (rectangles) and Ly-6c^{intermediate}/CD11b^{+} monocytes and granulocytes (ovals). Dot plots show one representative sample from $n = 9$ animals per condition (three per condition in each of three independent studies). Average percentages across all assayed samples are given in Fig. 3*C*.

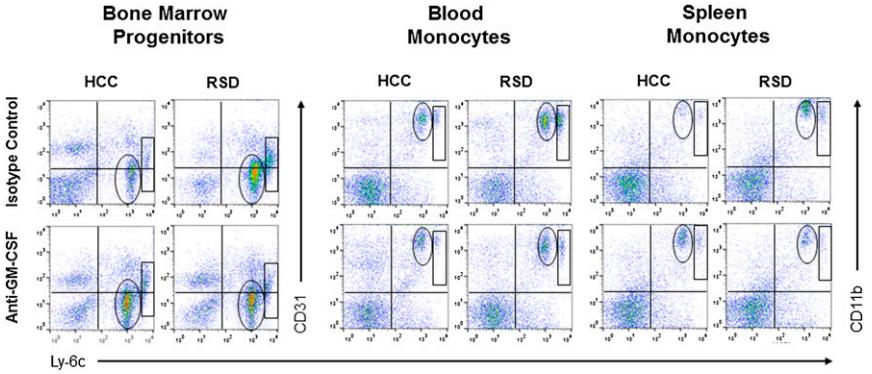

Fig. S2. Role of GM-CSF in RSD effects on monocyte and granulocyte prevalence. To determine whether RSD effects on myeloid cell prevalence were mediated by GM-CSF, mice received an i.p. injection of anti-mouse GM-CSF–neutralizing antibody MP1-22E9 or an equivalent volume of isotype control IgG2a κ antibody once every other day starting 24 h before experimental procedures. Following six cycles of RSD or parallel HCC conditions, (*i*) BMMCs (*Left*) were assayed by flow cytometry for prevalence of Ly-6c^{high}/CD31^{+} monocyte progenitors (rectangles) and Ly-6c^{intermediate}/CD31^{+} granulocyte progenitors (ovals) and (*ii*) PBMCs and total splenocytes (*Center* and *Right*) were assayed by flow cytometry for Ly-6c^{high}/CD11b^{+} monocytes (rectangles) and Ly-6c^{intermediate}/CD11b^{+} granulocytes (ovals). Dot plots show one representative sample from $n = 8$ animals per condition (pooled across three independent studies). Average percentages across all assayed samples are given in Fig. 3 *E* and *F*.

Other Supporting Information Files

Dataset S1 (XLS)
Dataset S2 (XLS)
Dataset S3 (XLS)
Dataset S4 (XLS)